PROPERTIES OF THE HYPERPOLARIZING-ACTIVATED CURRENT (i_f) IN CELLS ISOLATED FROM THE RABBIT SINO-ATRIAL NODE

By D. DiFRANCESCO, A. FERRONI, M. MAZZANTI AND C. TROMBA

From the Dipartimento di Fisiologia e Biochimica Generali, Università di Milano, via Celoria, 26, 20133 Milano, Italy

SUMMARY

1. Individual cells were isolated from the sino-atrial node area of the rabbit heart using an enzyme medium containing collagenase and elastase. After enzymatic treatment the cells were placed in normal Tyrode solution, where beating resumed in a fraction of them.

2. Isolated cells were studied in the whole cell configuration. Action potentials as well as membrane currents under voltage-clamp conditions were similar to those in multicellular preparations.

3. Pulses to voltages more negative than about -50 mV caused activation of the hyperpolarizing-activated current, i_f. Investigation of the properties of this current was carried out under conditions that limited the influence of other current systems during voltage clamp.

4. The i_f current activation range usually extended approximately from -50 to -100 mV, but varied from cell to cell. In several cases, pulsing to the region of -40 mV elicited a sizeable i_f. Both current activation and deactivation during voltage steps had S-shaped time courses. A high variability was however observed in the sigmoidal behaviour of i_f kinetics.

5. Plots of the fully-activated current–voltage (I–V) relation in different extracellular Na and K concentrations showed that both ions carry the current i_f. While changes in the external Na concentration caused the current I–V relation to undergo simple shifts along the voltage axis, changes in extracellular K concentration were also associated with changes in its slope. Again, a large variability was observed in the increase of I–V slope on raising the external K concentration.

6. The current i_f was strongly depressed by Cs, and the block induced by 5 mM-Cs was markedly voltage dependent.

7. Adrenaline (1–5 μM) and noradrenaline (1 μM) increased the current i_f around the half-activation voltage range and accelerated its activation at more negative voltages. Often, however, drug application failed to elicit any modification of i_f.

8. Current run-down was observed in nearly all cells, although at a highly variable rate. It was accelerated by raising the extracellular K concentration but did not show a marked use dependence. Both the i_f activation curve and the fully activated I–V relation were affected by run-down, the former being shifted to more negative values along the voltage axis and the latter being depressed with no apparent change of the

i_f reversal potential. This behaviour was interpreted as indicating that i_f availability depends upon the presence of an unidentified substance that is diluted by the pipette solution. The implication of this phenomenon and its possible relation to the properties of i_f in single sino-atrial node cells are discussed.

INTRODUCTION

The properties of the so called 'pace-maker' current, i_f, have been extensively analysed in cardiac multicellular preparations (Noble & Tsien, 1968; Peper & Trautwein, 1969; DiFrancesco 1981 a, b, 1982, 1984). Problems due to the multicellular nature of these preparations and to the related presence of extracellular cleft K accumulation/depletion phenomena, that had originally led to misinterpretations of the nature of this current system, have been overcome by dissecting pharmacologically the pace-maker current from other components that interfere with its time course during voltage-clamp pulses (DiFrancesco, 1981 a).

The recent development of techniques to separate cardiac cells (Powell & Twist, 1976; Taniguchi, Kokubun, Noma & Irisawa, 1981; Isenberg & Klöckner, 1982) have provided a new approach to the problem of isolating the current i_f from contaminating components. Indeed, although the possible presence of membrane infoldings may not allow a complete elimination of K accumulation/depletion, the lack of extracellular spaces separating contiguous cells is bound to reduce the interference of these processes in the time course of gated K-dependent components. Thus, in isolated Purkinje cells Callewaert, Carmeliet & Vereeke (1984) have demonstrated that the current recorded on hyperpolarization does not display the 'apparent' reversal that is seen in Purkinje fibres and that was responsible for the original misinterpretation of the current's ionic nature. Beside the reduction of interference from accumulation/depletion phenomena, the study of i_f in isolated cells has all the advantages of patch-clamp studies, among which are the control of the cell's intracellular as well as the extracellular ionic environment, the rapidity of solution changes and the elimination of all disturbances related to cell-to-cell communication.

In this paper we have investigated the properties of i_f in cells isolated from the sino-atrial node region of the rabbit heart, using the patch-clamp technique of Hamill, Marty, Neher, Sakmann & Sigworth (1981) in the whole-cell configuration. Our main aim was to confirm and possibly to extend previous observations of i_f in multicellular preparations, and also to verify whether the isolation procedure altered the i_f properties in single cells as compared to those in the intact tissue. We have indeed found that most of the known distinctive characteristics of i_f are present in this preparation, as they are in single Purkinje cells (Callewaert *et al.* 1984). However, we have also found some features of i_f behaviour which are new and different to those described in the multicellular preparations.

METHODS

Isolation of cells from the sino-atrial node area

Sino-atrial node preparations were made essentially as described in the previous literature (Noma & Irisawa, 1976; DiFrancesco, Noma & Trautwein, 1979; Brown & DiFrancesco, 1980). In brief, young albino rabbits weighing 1–1·5 kg were killed by a blow on the neck and rapid exsanguination.

The heart was quickly extracted and immersed in normal Tyrode solution containing heparin (Liquemin Roche: 0·4 ml/l) at room temperature (all solutions are described in Table 1). It was rinsed until clear of blood and put in pre-warmed (35 °C) Tyrode solution where, after removal of the ventricles, the sino-atrial node area was exposed and dissected out.

The atrial region surrounding the node was discarded and strips about 0·5–1 mm wide were cut perpendicularly to the crista terminalis border. The strips were left in warm solution gassed with O_2 for between 30 and 60 min, until regular contractions were observed (typically in more than 80% of strips). They were subsequently washed in nominally Ca-free, low-Mg solution (solution 2 in Table 1) and transferred to a test tube containing 5 ml of enzyme solution (3 in Table 1). Here the strips underwent a 'trituration' period of variable duration, ranging from 15 to 30 min. The 'trituration' device was adapted from the one used by Datyner, Gintant & Cohen (1985) for the isolation of Purkinje cells. The piston of a glass syringe was rigidly connected to a linear stepper motor (Airpax type L92141-P1, Airpax, Cheshire, CT, U.S.A.) whose driving unit was interfaced to a table HP–85 computer (Hewlett–Packard, San Diego, CA, U.S.A.)

Rhythmic movements of variable length, frequency and duration could then be generated by the computer. These were transmitted via tubing connexions to a pipette (5 mm orifice) immersed in the enzyme solution and resulted in controlled shaking of the strips. This method allows gentle agitation of the strips and is preferable to magnetic stirring because possible damage due to mechanical crushing is avoided. The shaking period lasted 15–30 min, according to individual preparations.

After treatment with digestion medium the cells were dispersed by a further trituration period in a high-K, low-Na, Ca-free and Mg-free solution containing albumin and nutritive compounds (solution 4 in Table 1). The use of a pipette with a smaller orifice (about 2 mm) and of faster shaking in this phase allowed a quicker and more efficient cell separation. After filtration through nylon mesh and addition of the same solution up to a final fixed volume (5 ml), the cells were left to sediment in a test tube. To increase the resistance to Ca, the Ca concentration was then increased in a step-like fashion up to 0·1, 0·2, 0·4 and 0·8 mM by addition, performed every 3 min, of the necessary amounts of either a solution containing 1·8 mM-$CaCl_2$ and 10 mM-NaCl, or normal Tyrode. All solutions contained albumin 1 mg/ml. Changes in the Ca, Na and K content were such that after four additions the above ion concentrations were 0·8, 58·7 and 17·1 mM, respectively. We found that this method yielded more satisfactory results than the use of enzyme solutions containing 200–250 μM-Ca (Powell, Terrar & Twist, 1980; Bendukidze, Isenberg & Klöckner, 1985). Following a suitable period of rest (10–20 min), the solution was then replaced by normal Tyrode containing albumin. The cells were stored at 4 °C and discarded after 24 h.

Using the method described above essentially two different types of cells were found. Cells of the type we have most frequently seen and on which the experiments here reported have been performed, have a very irregular, elongated shape, and some, but not all, have one or more thin prolongations protruding from the cell body. For this reason we shall refer to these as 'spider' cells. Their size is typically 40–50 μm in length and 10–15 μm in width. We have also found other cells which are bigger and have a more regular, rod-like shape with light striations. However, these cells only rarely possess a large i_t. Occasionally we also found round cells of the type described by Nakayama, Kurachi, Noma & Irisawa (1984). This latter type was observed more frequently in preliminary experiments where the solution used for cell separation following the digestion period was a high-K, low-Cl solution. As these authors describe, we found that several cells isolated with this method (and, in our hands, also partially damaged cells) tend to become round when kept in normal Tyrode solution long enough. We have found that, however, the cells where a large i_t is most frequently present belong to the 'spider' cell type.

Solutions

The solutions used for cell separation, cell external perfusion and pipette filling are described in Table 1.

Collagenase was purchased from Worthington Diagnostics, NJ, U.S.A. (Cls II). Adenosine 5′-triphosphate (ATP) was from Sigma, MO, U.S.A. (grade I, disodium or magnesium salt). In experiments where addition of adrenaline or noradrenaline was required, control and test solutions contained 0·5 mM-ascorbic acid to avoid autoxidation (Löffelholz & Scholz, 1970).

TABLE 1. Solutions used for cell dispersion, cell perfusion and pipette perfusion (concentrations in mM)

	Solution				
	1	2 Ca-free, low-Mg	3	4	5
	Tyrode	Tyrode	Enzyme	Dispersion	Pipette
pH	7·4	6·9	6·9	7·4	7·2
NaCl	140	140	140	—	10
KCl	5·4	5·4	5·4	20	—
CaCl$_2$	1·8	—	—	—	—
MgCl$_2$	1	0·5	0·5	—	—
KH$_2$PO$_4$	—	1·2	1·2	10	—
HEPES–NaOH	5	5	5	—	—
Glucose	10	10	10	10	—
Collagenase (mg/ml)	—	—	2	—	—
Elastase (μl/ml)	—	—	2·5	—	—
Albumin (mg/ml)	—	—	1	1	—
Glutamic acid	—	—	—	70	—
b-Hydroxibutyric acid	—	—	—	10	—
Taurine	—	50	50	10	—
HEPES–KOH	—	—	—	10	10
EGTA	—	—	—	—	1
ATP	—	—	—	—	2
Aspartic acid (K salt)	—	—	—	—	130

Current- and voltage-clamp procedures

Experiments were performed on single isolated cells dispersed on the surface of a small Petri dish, placed on the stage of an inverted microscope (Zeiss ID 02). After letting the cells sediment on the dish surface, normal Tyrode solution was perfused at a rate of about 2 ml/min. The dish volume was reduced to about 1 ml by inserting into it a stainless-steel conical ring of appropriate size, which thus allowed complete solution replacement every 30 s. Constant solution level was maintained by gentle suction. Together with inflow and outflow tubings, the Petri dish also contained a thermistor for temperature reading and reference Ag–AgCl pellet. The perfusing solution was pre-warmed by a Peltier device, and all experiments were performed at temperatures of 35–36 °C. After a variable time of perfusion with normal Tyrode the superfusing solution could be switched to a control one (usually containing 1 mM-BaCl$_2$ and 2 mM-MnCl$_2$) and then, when appropriate, to any required test solution. Solution changes were performed by use of miniature switchable electrovalves placed near the perfusion dish to minimize delays.

Whole-cell recordings (Hamill *et al.* 1981) were performed using pipettes with tip diameters of approximately 2–3 μm and with resistances ranging from 2 to 4 MΩ when filled with standard 'intracellular' solution (see Table 1). Pipettes were pulled from borosilicate glass capillaries (Jencons H 10) on a two-stage patch-pipette puller (Ochotzki, F.R.G.) and fire-polished. Current- and voltage-clamp experiments were performed using a patch-clamp amplifier built in our Department to Dr E. Wanke's design. In preliminary experiments we used an amplifier kindly sent to one of us by Dr A. Noma from Okazaki, Japan.

Data analysis

Voltage and/or current whole-cell traces and trigger pulses were recorded on an FM tape recorder during the experiments and played back for data analysis on an 8-bit digital oscilloscope (VUKO,

F.R.G.) interfaced to a desk HP–85 computer. This allowed 2 K or 8 K records to be stored on disk and, when required, plotted on a HP–7225B plotter. The results presented in this paper have been collected from thirty-two experiments where 205 cells were studied. Of these, 128 cells yielded successful whole-cell records of i_t.

RESULTS

General properties of cells isolated from the sino-atrial node region

The main aspects of the electrical behaviour of rabbit sino-atrial node cells have been described recently by Nakayama *et al.* (1984). Fig. 1 shows examples of action potentials recorded in single cells of the spider type. Although we did not make a
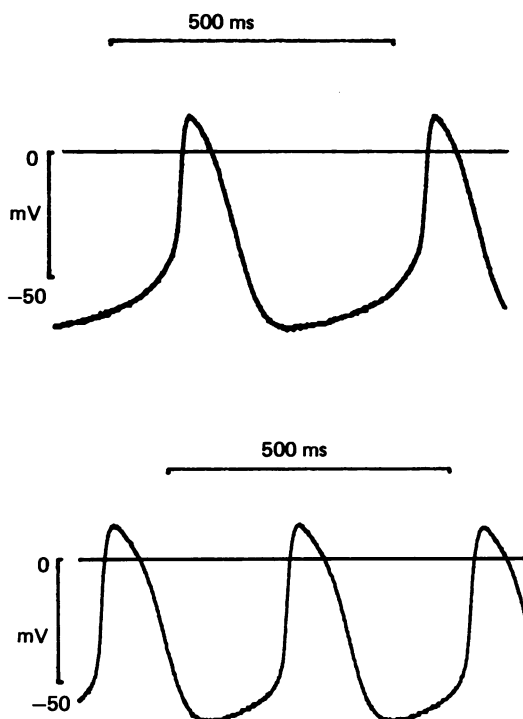
Fig. 1. Spontaneous activity recorded in cells isolated from the sino-atrial node region in normal Tyrode solution. The shape and size of action potentials and frequency of oscillation are comparable to those recorded in the intact tissue. Cells 20·1 (top) and 23·1 (bottom).

statistical analysis we often found that, at a visual inspection, a fraction of the apparently healthy cells (about 5–10 %) showed regular contractions. The fraction of contracting cells tended to increase during perfusion with Tyrode solution. However, rhythmic activity could not be easily recorded: out of the 205 cells used in this study, spontaneous action potentials could only be recorded in seven cells. This was essentially because: (a) successful seals on contracting cells were infrequent; (b) spontaneous activity often ceased after giga-seal formation or whole-cell penetration; (c) attempts to switch from voltage-clamp to current-clamp configuration often led

to arrest of beating cells. In Fig. 1, the action potential shape and size is comparable to that recorded by Taniguchi, Kokubun, Noma & Irisawa (1981), and to that normally seen in multicellular preparations (compare with Brown & DiFrancesco, 1980, Figs. 2, 5 and 6). In the experiment shown in Fig. 2A, whole-cell currents were
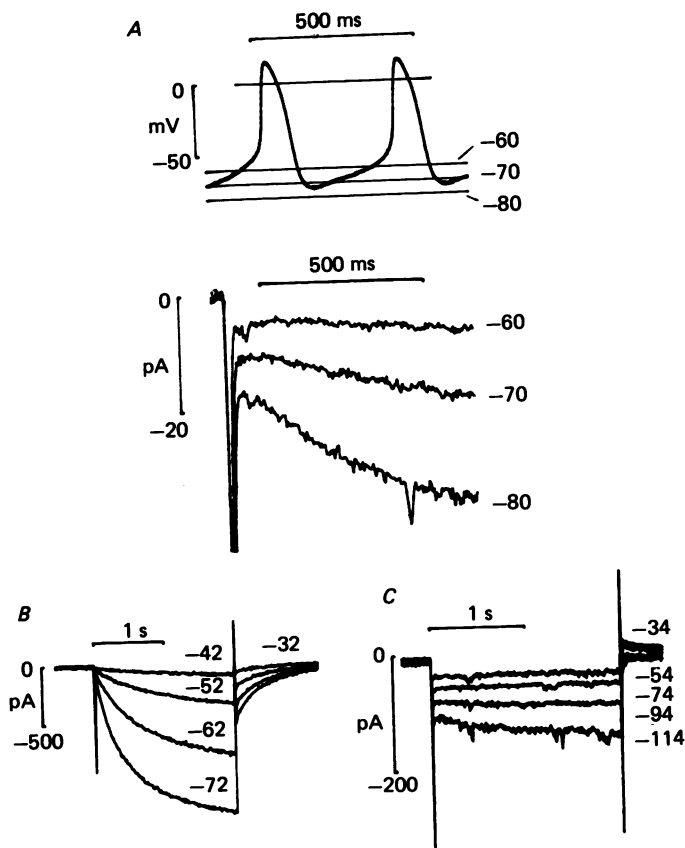

Fig. 2. Variability of i_f amplitude in single sino-atrial node cells. In A, the recording of spontaneous activity (top) was followed by voltage-clamp recording of i_f activation during pulses from a holding potential of -40 mV to the pace-maker range (-60 to -80 mV) as indicated. B and C, i_f records in two different cells of the 'spider' type. In B, 10 mV hyperpolarizations from -32 mV already activate i_f, which is by far the largest component present in all the voltage range investigated. In C, on the other hand, very little i_f is activated even at voltages as negative as -114 mV. Notice also the different ratio between time-dependent and time-independent components, and the noisier traces in C. Cells 23·1 (A), 26·8 (B) and 31·5 (C).

analysed during voltage-clamp hyperpolarizations from -40 mV in a cell where spontaneous activity had been previously recorded. Results similar to those shown in Fig. 2 were obtained in one further experiment.

As is known to occur in multicellular preparations, here, too, i_f develops during pulses that are within the range of diastolic depolarization. It is however important to stress that a feature of i_f as recorded in different cells was the variability of its

size and voltage activation threshold. This often occurred in the same experiment on apparently similar cells. Fig. $2B$, C shows two examples of current records from two cells of the same spider type where the full extent of current variability is apparent. While in some cells i_f does not activate even at voltages more negative than -100 mV (Fig. $2C$), in other cells it can be quite large and activated by small hyperpolarizations. For example in Fig. $2B$, i_f starts to be activated at -42 mV (see
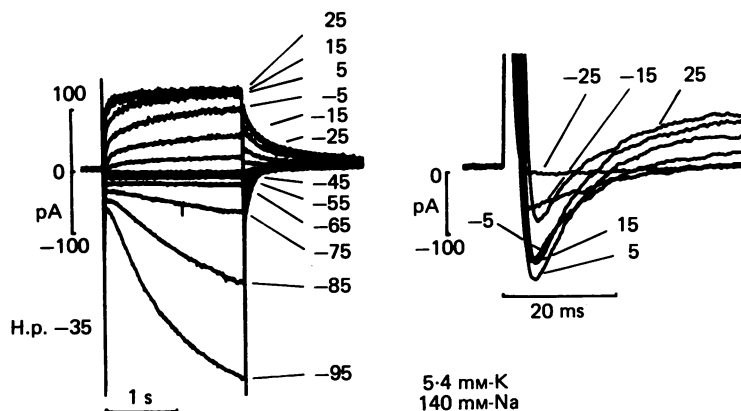
Fig. 3. Typical current records during pulses to the range -95 to 25 mV from a holding potential (h.p.) of -35 mV in a single sino-atrial node cell in normal Tyrode solution. The activation of i_K on depolarization and that of i_f on hyperpolarization are apparent in the left panel. The right panel shows activation of the slow inward current upon depolarization (same records of the left panel on an expanded time scale). Clamp potentials are indicated near corresponding traces. Cell 16·5.

tail on return to the holding potential of -32 mV). This observation may have some relevance to the issue of the importance of i_f in controlling the pace-maker depolarization phase (DiFrancesco, 1985). This variability is likely to be linked to another property of i_f in single cells, its time-dependent run-down, which is discussed later.

Fig. 3 illustrates a typical example of current records elicited during pulses applied from a holding potential of -35 mV in a single cell. Depolarizations activate the slow inward current (i_{si}: see right panel of Fig. 3) and the slower outwardly directed current i_K, whose deactivation tails appear on repolarizing to the holding potential (left panel). Hyperpolarizations, on the other hand, activate i_f. Leakage and time-independent components are small in the voltage range investigated, in accordance with the data in multicellular sino-atrial node preparations (Noma & Irisawa, 1976; Noma, Yanagihara & Irisawa, 1977; Brown & DiFrancesco, 1980; Yanagihara & Irisawa, 1980).

Properties of i_f

We have further investigated the properties of i_f in single nodal cells in order to establish similarities and possible differences with its properties in multicellular preparations and in single Purkinje cells (Callewaert *et al.* 1984). Several experiments
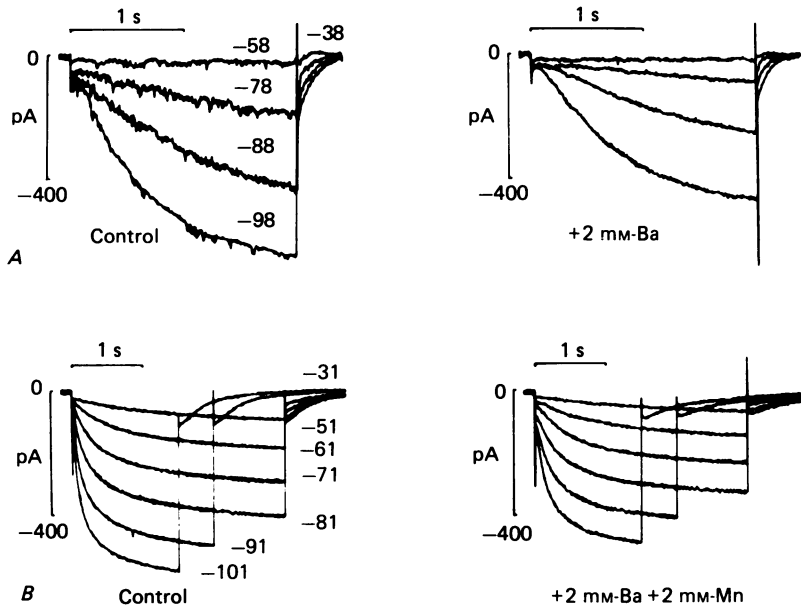
Fig. 4. i_f records before (A, left) and after (A, right) addition of 2 mM-$BaCl_2$ and, in another cell, before (B, left) and after (B, right) addition of 2 mM-$BaCl_2$ and 2 mM-$MnCl_2$. Voltages during pulses are marked near corresponding traces in the left panels. Holding potentials were -38 (A) and -31 mV (B). Addition of the divalent cations gives rise to a small current decline. Notice the reduction of current fluctuations after Ba in A. Cells 18·3 (A) and 22·4 (B).

were made in the presence of $BaCl_2$ (1–2 mM) and $MnCl_2$ (2 mM) to improve the resolution of the i_f time course during both activation and deactivation (see DiFrancesco, 1981 b). Fig. 4 shows that addition of Ba reduces, as expected, the interference of K-dependent currents (i_{K1} and i_K : i_{K1} is in any case much smaller here than in Purkinje fibres). Addition of Mn was used to reduce the slow inward current i_{si} on return from hyperpolarizations. We added Mn routinely even if this component did not always appear to be large enough to interfere seriously with the recording of i_f decay on repolarization, as apparent in Fig. 4B, left. An additional beneficial effect that we have sometimes observed on adding Ba was the decrease of membrane current fluctuations apparent during negative pulses (see Fig. 4A), and possibly again

Fig. 5. i_f activation curve in three different cells. 1 mM-$BaCl_2$ and 2 mM-$MnCl_2$ present in all cases in the extracellular solutions. The protocols (see upper left records in each panel) consisted of test pulses to various voltages (labelled near corresponding traces) followed by deactivating positive (A and B) or extra-activating negative (C) pulses to fixed voltages. Lower-left traces in each panel represent, on expanded time-scales, the actual decay tails (A and B) or the extra-activation records (C) elicited on stepping to 17 (A), 6 (B) and -125 mV (C) from the voltages indicated near each trace. In A and B plotted values represented the decay tail amplitudes and in C the differences to the maximal current amplitude at -125 mV. Notice that while the degree of activation in B and C extends approximately over the range -50 to -100 mV, in A i_f begins to activate at voltages more positive than -43 mV. Cells 35·5 (A), 33·6 (B) and 33·8 (C).
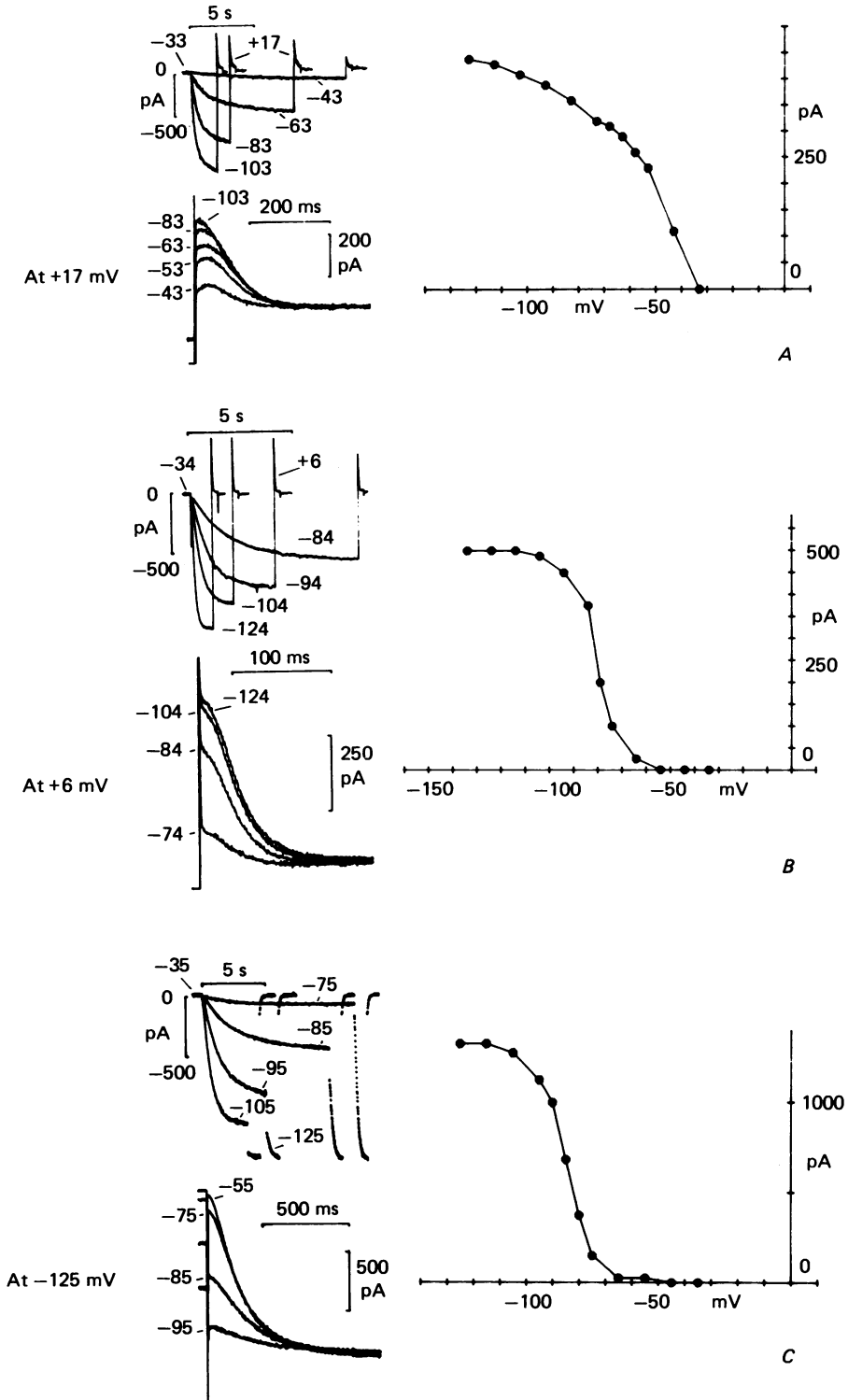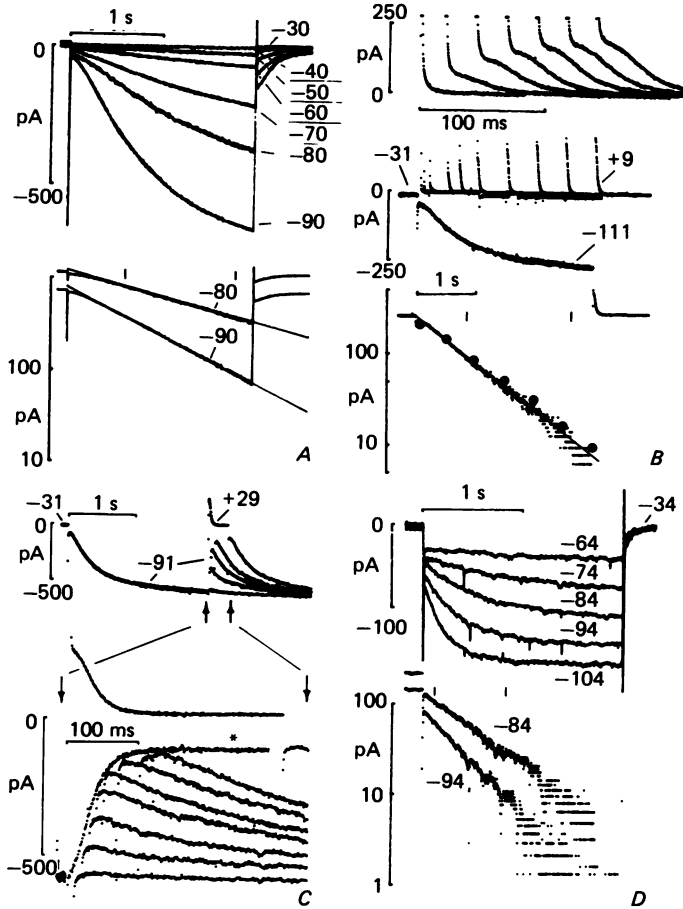
Fig. 5. For legend see opposite.

Fig. 6. Kinetic properties of i_f in single sino-atrial node cells. *A*, activation of i_f displaying a sigmoidal time course in both linear (top) and semilogarithmic plots (bottom) during hyperpolarizations from -30 mV to the range -40 to -90 mV, as indicated. In the bottom panel, straight lines were obtained by least squares fitting of experimental points (between times marked by vertical bars). Time constants were 1·634 (-80 mV) and 0·847 s (-90 mV). Cell 22·1. *B*, envelope test during activation at -111 mV. From -31 mV, hyperpolarizing steps of variable duration to -111 mV were followed by 1 s steps to 9 mV (middle panel). Tails at 9 mV are plotted on an expanded time scale in the top panel, so that the starting position of each trace corresponds with that of the same trace in the middle panel. The bottom panel shows semilogarithmic plots of current onset at -111 mV and, after appropriate vertical shift, of tail amplitudes (dots). Fitting of the current onset between times marked by bars (straight lines) yielded a time constant of 0·847 s. Cell 30·4. *C*, envelope test during deactivation at 29 mV. After current activation at -91 mV, pulses to 29 mV of variable duration were followed by re-activating steps to -91 mV (see protocol in the top panel). Re-activation records and tail at 29 mV are shown on a larger time scale in the bottom panel. The tail at 29 mV was also replotted after appropriate scaling (trace marked by asterisk) to better compare its sigmoidal time course with that of the re-activation records envelope. Cell 32·2. *D*, example of i_f records showing no delay in current activation. This is apparent from both linear (above) and semilogarithmic plots (below: steps to -84 and -94 mV). Time constants (fitting between bars) were 0·500 (-84 mV) and 0·368 s (-94 mV). Notice the presence of a large leakage and of large current fluctuations. Cell 13·1. Extracellular solutions were normal Tyrode in *A* and *D*, and normal Tyrode containing 1 mM-$BaCl_2$ and 2 mM-$MnCl_2$ in *C* and *D*.

related to K-dependent conductance systems that are blocked by Ba. As apparent in Fig. 4, the addition of Ba and Mn often decreased the size of i_t recorded on hyperpolarization. We have not investigated this effect, which has been previously observed in Purkinje fibres (DiFrancesco, 1981b; Cohen, Falk & Mulrine, 1983) but apparently not in single Purkinje cells (Callewaert et al. 1984).

Current kinetics

The variability of i_t magnitude in different cells and the phenomenon of current run-down (this point is further developed below) make a quantitative analysis of i_t kinetics impossible. We have therefore limited our observations to the qualitative features of the current time course during activation and deactivation.

Fig. 5 shows three examples of activation curves for i_t in three different cells. The curves can be reconstructed using two protocols, which essentially consist of test pulses followed by pulses to either the bottom (Fig. 5A and B) or the top (C) of the i_t activation range, where the current amplitude is measured. In Fig. 5B and C the current activation extends approximately over the range −50 to −100 mV, which is similar to that reported in multicellular sino-atrial node preparations (Yanagihara & Irisawa, 1980). In the experiment of Fig. 5A, however, i_t appears to be activated at more depolarized voltages. Indeed, stepping to −43 mV results in a substantial current activation, which is reflected by the size of the decay tail on stepping from −43 to 17 mV (Fig. 5A, left panel). The results of Fig. 5 may reflect, as mentioned in relation to the plots in Fig. 2, a natural variability of the i_t range of activation. Some of this variability, however, may also be attributed to the run-down phenomenon that is described below.

One of the most remarkable aspects of i_t kinetic behaviour in Purkinje fibres is the presence of a sigmoidal time course during both onset and decay (DiFrancesco & Ferroni, 1983; DiFrancesco, 1984). Fig. 6A, B shows that on activation this property is shared by i_t in the isolated sino-atrial node cell both in the absence (A) and in the presence of Ba (B). The same behaviour has also been reported by Callewaert et al. (1984) in single Purkinje cells.

The sigmoidal time dependence of onset is made more evident by drawing semilogarithmic plots of the current records (Fig. 6A), or by the use of the envelope test as shown in Fig. 6B. Furthermore, in the presence of Mn, which allows a better resolution of i_t deactivation, the envelope test performed on depolarization shows that the current decay is S-shaped, too. This is shown in Fig. 6C, where the i_t deactivation at 29 mV and the envelope of re-activation records at −91 mV can be seen to display a similar, sigmoidal time dependence. Although the delay in current activation during negative and that of current deactivation during positive voltage pulses are often, as in Purkinje fibres, very pronounced, we have found a remarkable variability in this feature of i_t kinetics, too. Fig. 6D shows a set of current records during hyperpolarizations to the range −64 to −104 mV where both linear and semilogarithmic plots fail to reveal substantial delays in current activation. Indeed, the current time course is best approximated by single-exponential curves, as apparent from the plots of the −84 and −94 mV records in the lower panel of Fig. 6D. The behaviour in Fig. 6D was rarely observed. However we found that the delay in current activation during a fixed step and, more generally, the kinetic properties of
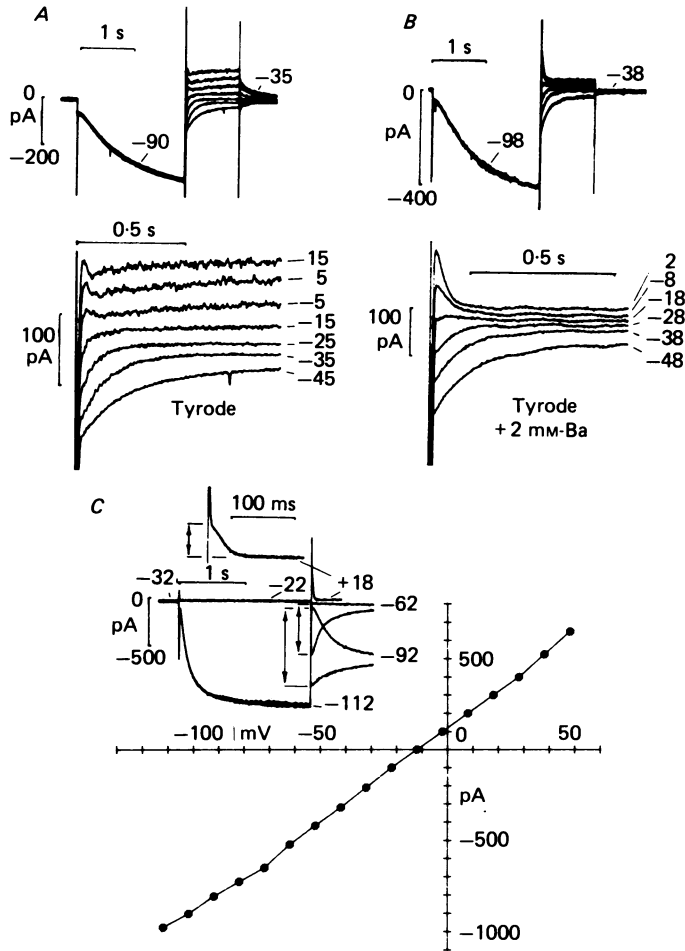
Fig. 7. *A*, *B*, i_f current reversal measured in normal Tyrode (*A*) and, another cell, in the presence of 2 mM-BaCl$_2$ (*B*). Following activation, i_f was deactivated by 1 s depolarizing steps to various voltage levels, according to protocols shown in the top panels. The expanded decay tails plotted in the bottom panels show that the i_f reversal lies between -5 and -15 mV in *A*, and at about -18 mV in *B*. Notice in *A* that activation of i_K overlaps i_f decay and that the traces are noisier. Both these features are absent from the records in the Ba-containing solution in *B*. Cells 16·5 (*A*) and 18·3 (*B*). *C*, fully activated *I–V* relation, $\bar{\imath}_f(E)$. The protocol used to measure it is shown in the inset, and consisted of pairs of pulses to either the top (-22 mV) or the bottom (-112 mV) of the current activation range, followed by steps to test potentials. The difference between starting values of the traces at the same test voltage (arrows) represents $\bar{\imath}_f$ at that voltage (see DiFrancesco, 1981*b*, Fig. 1). The current decay at 18 mV is also shown on a faster time scale (top trace). Line drawn through experimental points. Cell 26·8.

i_f were not always stable but tended to vary with time. This aspect of i_f behaviour is more fully investigated below (Figs. 12–15).

Ionic nature of i_f

In both the sino-atrial node (Brown & DiFrancesco, 1980; DiFrancesco & Ojeda, 1980) and the Purkinje fibre (DiFrancesco, 1981*b*), i_f has been shown to be carried
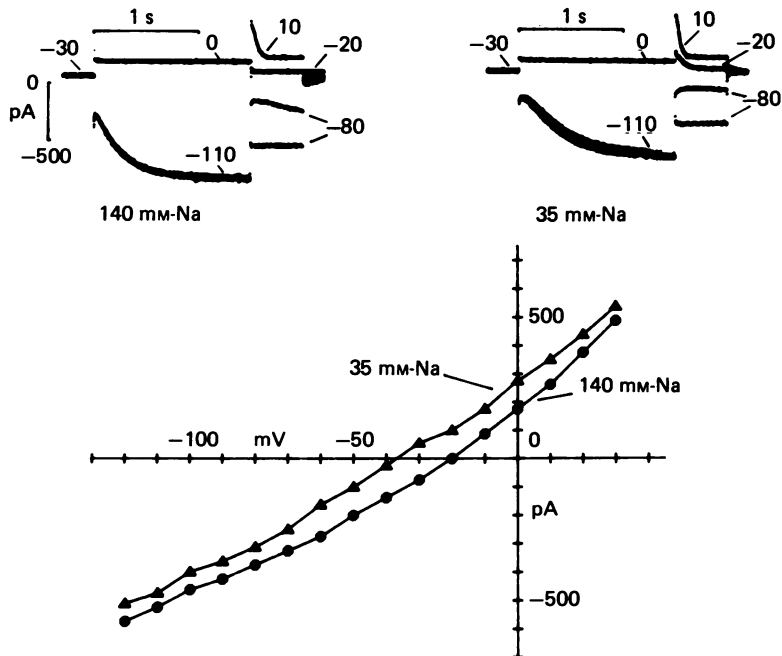
Fig. 8. Effect of lowering the external Na concentration from 140 to 35 mM (choline used as a substitute) on the $\bar{i}_f(E)$ curve. As in Purkinje fibres (DiFrancesco, 1981b), the main effect of Na reduction is a negative shift of the I–V relation along the voltage axis. The insets show actual current records at the normal (left) and low external Na concentration (right) at the voltages indicated (see protocol in Fig. 7C). Comparison of the control trace at −20 mV (pulse from −110 mV) with that after Na replacement clearly indicates that a shift of the current reversal potential has occurred. Lines drawn through points. Cell 30·9.

by Na and K. Results consistent with the mixed ionic nature of i_f have also been obtained in the sheep atrium (Earm, Shimoni & Spindler, 1983), in the isolated Purkinje cell (Callewaert et al. 1984) and in other tissues where i_f has been found (for example, Halliwell & Adams, 1982; Mayer & Westbrook, 1983; Bader & Bertrand, 1984). Panels A and B of Fig. 7 show current records during protocols used to determine the voltage at which i_f reverses. They consist of a series of fixed hyperpolarizing pulses followed by depolarizations to various levels.

In the absence of Ba (Fig. 7A), i_f deactivation overlaps activation of i_K (see the i_K tails on return to −35 mV in the upper panel of Fig. 7A) and the current reversal is revealed by the appearance of a relatively fast outward-decreasing transient following the capacitative surge at voltages more positive than −5 mV. Also, current fluctuations are large. In the presence of Ba, on the other hand, both current fluctuations and i_K are depressed and the i_f decay is much better resolved (Fig. 7B). In both the cases illustrated in Fig. 7 the current reverses in the expected range for the Na and K concentration used (Fig. 7A: −15 to −5 mV; B: around −18 mV; compare for example with Purkinje fibre data, DiFrancesco, 1981b, Fig. 11). More complete information on the ionic nature of i_f can be obtained by plotting its fully-activated current–voltage (I–V) relation, as shown in Fig. 7C. The voltage
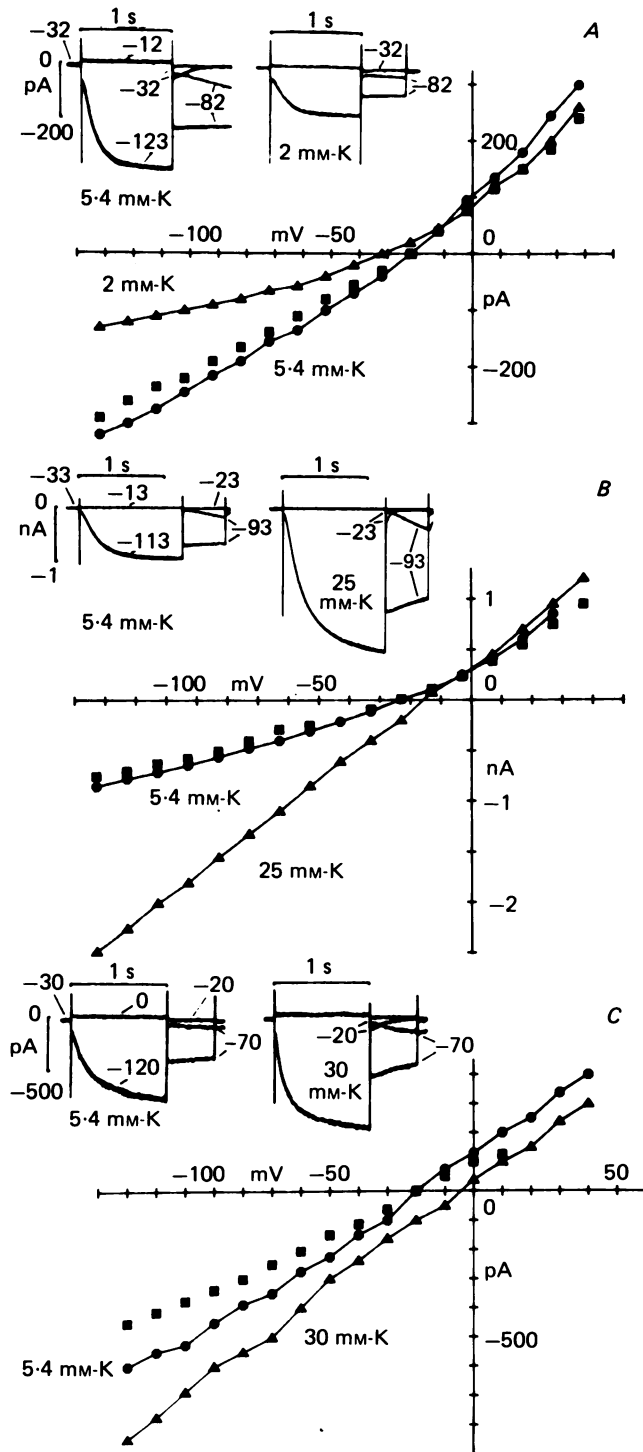
Fig. 9. For legend see opposite.

protocol is similar to that used in Purkinje fibres (DiFrancesco, 1981 b) and allows a satisfactory resolution of the amplitude of i_f over a relatively large voltage range (about -110 to $+50$ mV in the case of Fig. 7C). The current reversal extrapolated from the I–V curve occurs at -12 mV, and is again in agreement with previous data.

Results from an experiment where the effects of extracellular Na on i_f were studied are reported in Fig. 8. Actual current records used to reconstruct the fully activated I–V relation (top panels in Fig. 8) show that lowering the external Na concentration from 140 to 35 mM causes the current to become more outward at all voltages, and that the current reversal shifts from -20 to about -37 mV. Plotting the $\bar{i}_f(E)$ relations (bottom panel in Fig. 8) reveals that the effect of lowering the external Na concentration is, as in Purkinje fibres (DiFrancesco, 1981 b), essentially that of shifting the I–V curve to more negative voltage levels. Results similar to those reported in Fig. 8 have been obtained in three further experiments where the Na concentration was lowered from 140 to 35 mM.

Besides carrying it, in Purkinje fibres K ions have been shown to have an activation-like effect (DiFrancesco, 1982) on i_f, when added extracellularly. A large current increase on raising extracellular K has been reported in the sino-atrial node, too (Brown & DiFrancesco, 1980; DiFrancesco & Ojeda, 1980: Maylie & Morad, 1984). We have observed a similar effect of K on i_f in the isolated sino-atrial node cell. Fig. 9 shows the results from three experiments where the external K concentration was changed from 5·4 mM to 2 (A), 25 (B) and 30 mM (C). The insets show current traces during protocols like that illustrated in Fig. 7C, recorded at the K concentrations indicated. Changes in i_f size, particularly at the voltages where in each of the three cases i_f reversed at the lower K concentration (Fig. 9A: -32 mV at 2 mM-K; B: -23 mV and C: -20 mV at 5·4 mM-K), are clearly visible. In all cases both the reversal potential and the slope of the I–V curve change in the direction expected from the known activation-like effect of K. The action of K is however very variable, as can be judged by comparing the data in panel B with those in panel C. Indeed, in the latter case raising K causes only a minor increase of the maximal i_f conductance, and no cross-over of I–V curves. The reason for this discrepancy may be the current run-down that occurs, although to a highly variable degree, in all cells. This feature of i_f is treated in some detail below. Here it may be sufficient to mention that evidence for a current run-down comes from the comparison of the I–V plots on return to the original K concentration (squares) with the control ones (circles). Indeed, a slope reduction occurs in all three cases, and is most pronounced in panel C of Fig. 9. We interpret this as reflecting the degree of current reduction occurring

Fig. 9. Effects of changes in the external K concentration on $\bar{i}_f(E)$. In three different experiments, the fully-activated I–V relation was measured in a control 5·4 mM-K solution (●), in a test solution containing 2 (A), 25 (B) or 30 (C) mM-external K (▲), and after return to control (■). In each panel, insets show actual current records at the voltages indicated. Changes in the current reversal potentials and in the slope of I–V curves are in the same direction as in Purkinje fibres (DiFrancesco, 1981 b). In C, however, the increase in I–V slope was smaller than expected for an increase from 5·4 to 30 mM-K, and no cross-over was observed. Notice that the I–V relations measured after return had in all cases a reduced slope as compared to control, and that this decrease was larger in C. Lines drawn through points. Cells 32·3 (A), 33·5 (B) and 30·3 (C).

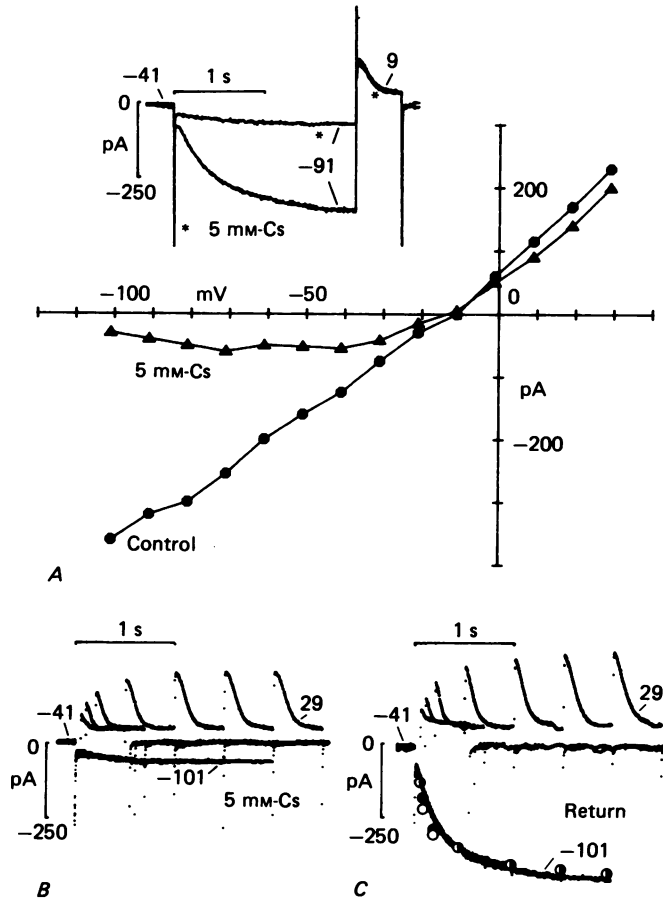Fig. 10. Cs-induced block of i_f. A, fully-activated $\bar{i}_f(E)$ relation in a control solution (containing 2 mM-BaCl$_2$ and 2 mM-MnCl$_2$) and after addition of 5 mM-CsCl. The voltage dependence of block is apparent from the outward-rectifying shape of the I-V curve in the presence of Cs. The inset shows records during 2 s pulses to −91 mV followed by 0·5 s pulses to 9 mV from a holding potential of −41 mV before and after (*) addition of Cs. The current is hardly altered at 9 mV, but is markedly depressed at −91 mV. B and C, envelope tests at −101 mV performed during perfusion with Cs (B) and after return to control (C). The tests were performed by applying activating pulses of variable duration to −101 mV, followed by 500 ms deactivating pulses to 29 mV (see Fig. 6B above). After scaling up to the current size at −101 mV, the amplitudes of tails in the presence of Cs (open circles) and after return to control (filled circles) are also plotted in C. The onset of inward current and the envelope of outward tails follow similar time courses, indicating that Cs has little effect on the i_f kinetics. Cell 27·1.

during the experiment (see Fig. 12). Regardless of the current run-down phenomenon, results demonstrating a K-induced activating action on i_f have been obtained in sixteen cells where the K concentration range 2–30 mM was investigated.

Block induced by extracellular Cs

We have qualitatively investigated the action of extracellular Cs on i_f in experiments as that shown in Fig. 10. As reported for i_f in Purkinje fibres (DiFrancesco, 1982)
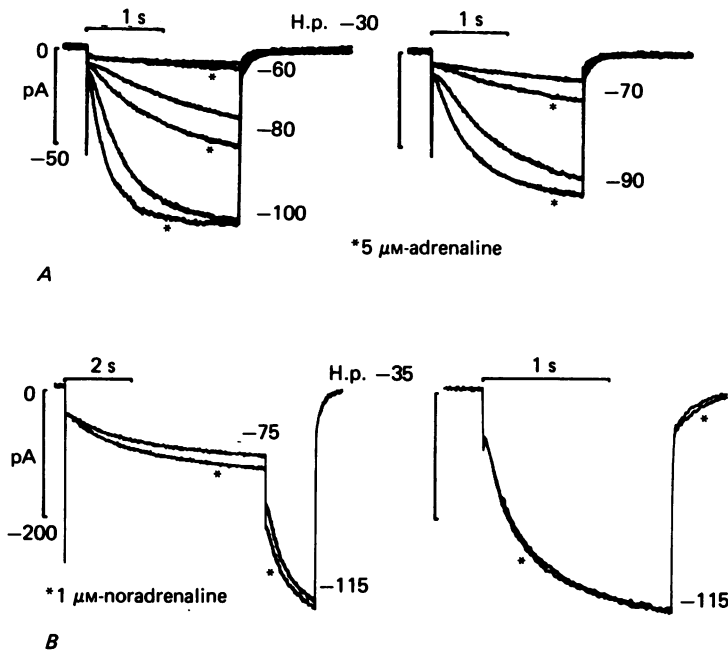
Fig. 11. Effect of adrenaline (A) and noradrenaline (B) on i_f. In A, current traces during voltage clamp pulses from −30 mV to the range −60 to −100 mV, as indicated, are shown before and during (*) perfusion with 5 μM-adrenaline. Adrenaline increased the speed of current onset at voltages more negative than −80 mV, but the current amplitude on stepping to −100 mV was not increased by the drug, as expected from an alteration of the current activation rate and not of its fully activated size. Cell 33·18. B (left), current records during 5 s steps from −35 to −75 mV followed by 1·5 s steps to −115 mV before and after (*) perfusion with 1 μM-noradrenaline. Notice the larger current onset at −75 mV in the presence of the drug. B (right), current records during pulses to −115 mV which have not been preceded by a prepulse, plotted on a faster time scale. Noradrenaline (*) causes a minor acceleration at −115 mV, but no increase of i_f. It also slightly decelerates the current decay on return to −35 mV. Cell 35·7. In both experiments the extracellular solution was normal Tyrode.

and in Purkinje cells (Callewaert *et al.* 1984), Cs blocks the i_f channel and the block is voltage dependent. The inset in Fig. 10A shows that the addition of 5 mM-CsCl nearly fully abolishes the current activated on hyperpolarizing to −91 mV, while the current tail recorded on depolarizing to 9 mV is almost unaltered. The voltage dependence of the Cs-induced block is made more evident by plotting the fully activated I–V relations in the absence and in the presence of Cs. These are shown in Fig. 10A. Possible effects on the i_f kinetics at potentials where the current was suppressed by Cs were checked by performing envelope tests during and after perfusion with 5 mM-Cs, as shown in Fig. 10B and C, respectively. Disregarding a slight acceleration of the envelope of tails in the presence of Cs (open circles in Fig. 10C) as compared to control conditions (filled circles), the envelopes of tails at 29 mV follow a time course similar to that of the current onset at −101 mV (in the control solution), which excludes gross alterations of the i_f activation kinetics induced by Cs in this case. We have not investigated the concentration and voltage dependence of the Cs-induced block of i_f in the sino-atrial node cell. However, it should

be mentioned that the blockade caused by Cs in the experiment of Fig. 10 appears less marked than that expected from the Purkinje fibre's data (compare, for example, with Figs. 2 and 9 of DiFrancesco, 1982). A blocking action less efficient than in Purkinje fibres was also observed in two more cells after addition of 1 mM-Cs.

Effect of adrenaline

Adrenaline increases i_f during hyperpolarizations toward the half-activation range and accelerates its activation rate during larger negative pulses. This is shown in Fig. 11 A for an experiment where adrenaline at the concentration of 1 μM was added to the control (normal Tyrode) solution. The time course of the current recorded on pulsing to voltages more negative than -80 mV was accelerated, and the current size increased in the range near -70 mV. It may be noticed that at -100 mV the current amplitude is not increased by adrenaline, which is consistent with the view that the neurotransmitter acts on the current kinetic parameters rather than on the fully activated current size (Tsien, 1974a).

A similar observation applies to the experiment shown in Fig. 11 B. The records shown on the left were obtained by applying voltage pulses to -115 mV, preceded by pulses to -75 mV, before and just after addition of 1 μM-noradrenaline. The drug-induced increase in magnitude on stepping to -75 mV was accompanied by a decrease of the current size at -115 mV. This was caused by a shift of the i_f activation curve, however, rather than changes in the current fully activated amplitude, as the current size during a pulse from -35 to -115 mV (that is, a pulse spanning the whole activation range) did not vary after noradrenaline (Fig. 11 B, right). Notice also that the current decay at -35 mV was slightly slower during drug application, which is also consistent with a positive shift of current kinetics at depolarized voltages. Results similar to those in Fig. 11 have been obtained in twelve more experiments on different cells. Also, a shift of the i_f activation curve after adrenaline has been clearly observed in single Purkinje cells (Callewaert *et al.* 1984). However, we have more often observed that addition of either adrenaline (1–5 μM) or noradrenaline (1 μM) resulted in no appreciable effect on i_f. Out of thirty-four cells where either drug was applied, only twelve cells gave positive results immediately after drug application, while twenty-two cells did not respond as expected. An even more negative result was obtained when studying the effects of drug application on the i_f activation curve. We found that the curve was displaced toward more positive voltages, as expected, in only one out of twelve experiments where either adrenaline or noradrenaline was used. A possible explanation for these inconsistent results is again related to the run-down phenomenon described below. Indeed, as shown in Fig. 15, run-down can affect dramatically the position of the i_f activation curve.

Current run-down

One of the most serious problems that we have faced in trying to establish the effects, shown above, of agents like extracellular K, Na, Cs and adrenaline, was the evidence that the current size tended to diminish in the course of the experiments. This is visible for example in the experiments of Fig. 9. The current time-dependent reduction was a frequent finding, but its extent varied considerably from cell to cell and in some cases was hardly noticeable. Although its development was often very
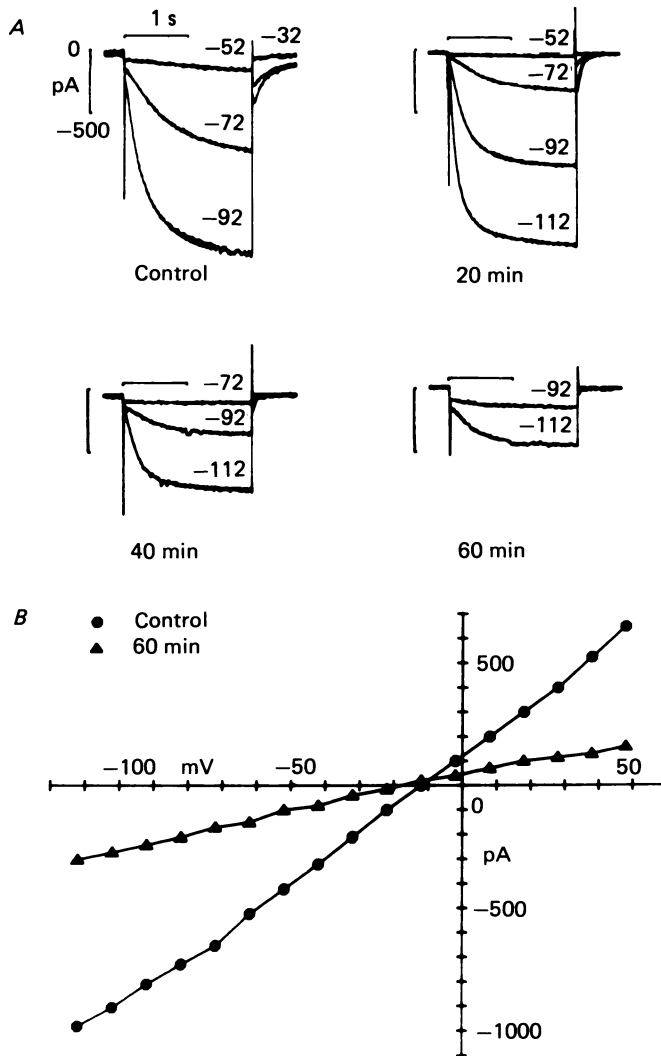
Fig. 12. Current run-down. *A*, i_f records during steps to the voltages marked near corresponding traces at the beginning of the experiment (control) and after various times as indicated. *B*, fully activated *I–V* relations at the beginning of the experiment (●) and after 1 h (▲), showing that the current run-down is associated with a slope decrease but with no change of the i_f reversal potential. Cell 26·8.

irregular, in our experiments we tended to use, particularly when a constant reference was essential, only cells where the current was apparently stable with time, and discarded all results that were obviously affected by heavy current deterioration. In this section we report evidence concerning this phenomenon. Fig. 12 shows sets of current traces recorded in a cell at various times during perfusion with normal Tyrode.

The current activated on stepping to the range −52 to −112 mV became evidently smaller after 20 and 40 min, and had nearly disappeared after 60 min perfusion. In Fig. 12 *B*, plots of the $\bar{i}_f(E)$ relations at the beginning of the experiment and after
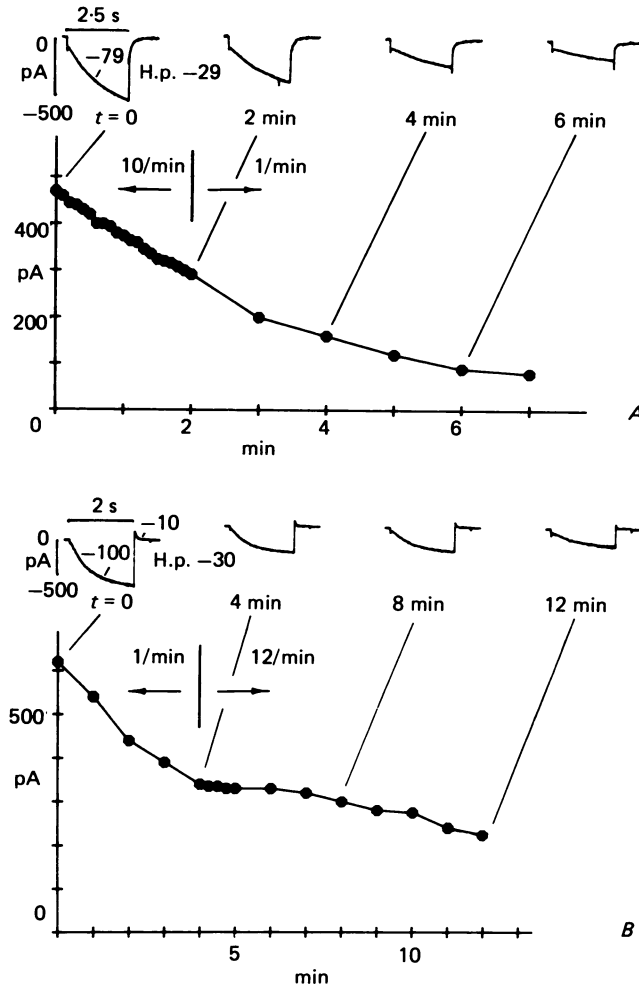
Fig. 13. Lack of use dependence of run-down. In A, 2·5 s pulses to -79 mV from a holding potential of -29 mV were delivered every 6 s for the first 2 min, and then every 1 min. The graph shows the current amplitude during activation as a function of time. Current records at 0, 2, 4, and 6 min from the beginning of the experiment are shown in the top part of the panel. Cell 35·1. In B, 2 s pulses to -100 mV, followed by 0·5 s pulses to -10 mV, were applied from -30 mV every minute for the first 4 min, and every 5 s from the 4th to the 12th min. The graph reports the current amplitude at -100 mV as a function of time. This was recorded every 15 s from the 4th to the 5th min, and only every minute thereafter. Cell 32·4.

1 h reveal that the current run-down is associated in this case with a change of the I–V relation slope, while the reversal potential does not vary. Thus, this phenomenon appears to be caused by a reduced availability of conducting channels.

A run-down process has been reported for Ca currents in the snail neurones (Byerly & Hagiwara, 1982) and in chromaffin cells (Fenwick, Marty & Neher, 1982), and has been shown to be accelerated by processes that increase the Ca concentration at the intracellular side of the membrane. A possible cause for the i_f run-down process is,
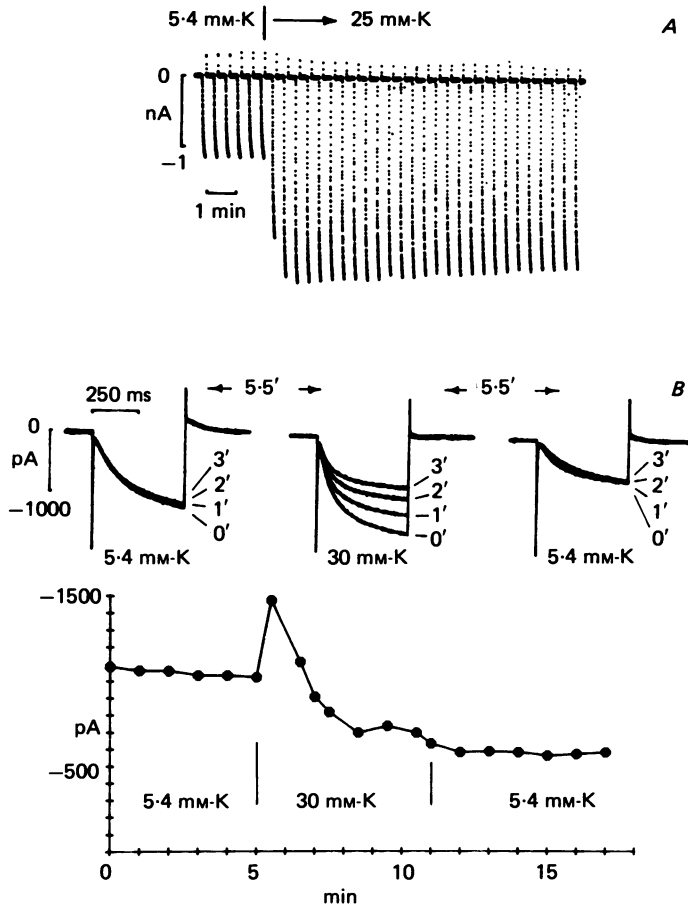
Fig. 14. Effect of external K on run-down. A, continuous recording of current during repetitive 2 s pulses from -30 to -100 mV, followed by 0·5 s pulses to 0 mV. Raising the extracellular K concentration from 5·4 to 25 mM gives rise to the expected current increase, but also increases the rate of run-down, as apparent from the decline in current amplitude. Cell 33·2. B (bottom), plot of the current amplitude in the course of an experiment where the extracellular K concentration was changed from 5·4 to 30 and then back to 5·4 mM. Dots indicate the current size during 0·5 s hyperpolarizations to -108 mV from a holding potential of -28 mV, taken every minute. The expected current increase is followed by a rapid run-down that brings the i_f size down to values lower than in control. The top panel shows current records at 0, 1, 2 and 3 min after the beginning of the experiment (left) or after K replacement (middle: 5·5 min and right: 11 min after start of experiment). During perfusion with high K the current run-down is obviously much faster. Cell 29·7.

as suggested for the Ca current in chromaffin cells, the dependence of the channel availability on the presence of a substance that is diluted by the pipette solution and diffuses out of the cell in the whole-cell configuration. To check whether the i_f deterioration during whole-cell recording in sino-atrial node cells is dependent on channel activation, we applied trains of hyperpolarizing pulses with different frequency rates, as shown in Fig. 13. These experiments do not provide clearcut evidence that the rate of current run-down depends upon the frequency of current
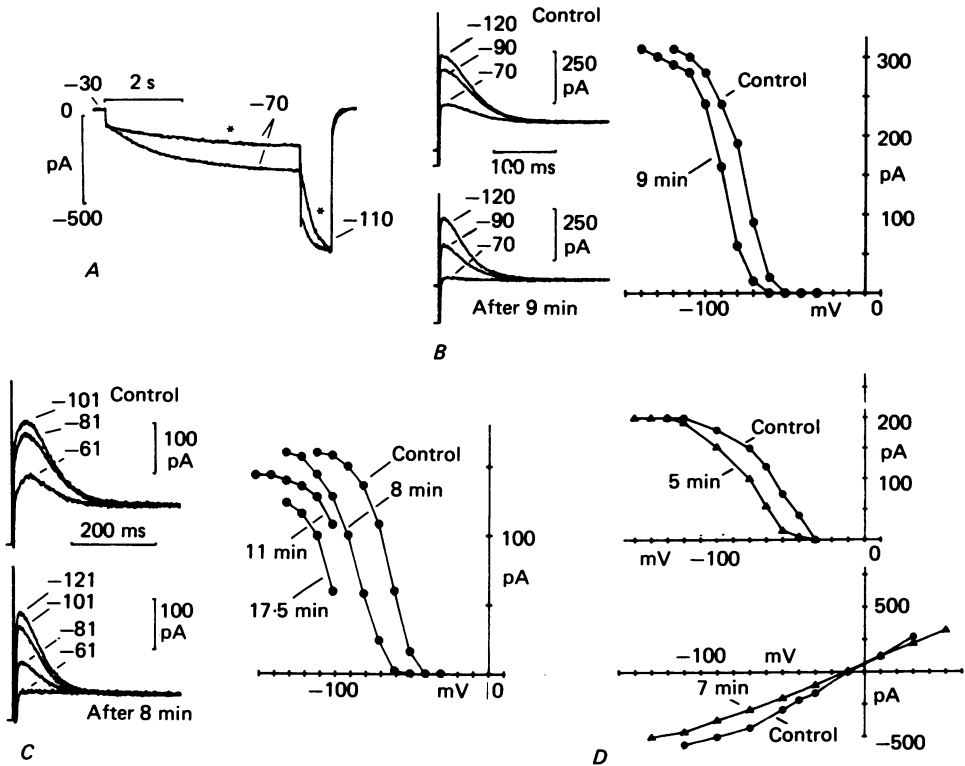
Fig. 15. Modifications of i_f kinetics during run-down. *A*, i_f records during 5 s steps from -30 to -70 mV followed by 1 s steps to -110 mV at the start of the experiment and after 1 min (*). The large reduction at -70 mV is compensated by an increase at -110 mV, as if the current run-down had caused only a negative shift of the activation curve voltage dependence (compare with Fig. 11*B*). Cell 36·9. *B*, activation curve measured at the start of the experiment (control) and after 9 min, showing that a negative shift has occurred during run-down without obvious change in the current size at 10 mV. Tails on the left were recorded at 10 mV on pulsing from the voltages indicated (same protocol as in Fig. 5*A*, *B*). Cell 37·4. *C*, activation curve measured at the start of the experiment (control), after 8 min and partially after 11 and 17·5 min, as indicated. On the left, tails recorded at $t = 0$ (control) and after 8 min at 9 mV from the voltages indicated show that the i_f activation range has moved to more negative potentials (compare for example the -61 mV tail at $t = 0$ with that at $t = 8$ min). Also notice that, as in *B*, the current decay is faster after run-down. This is the expected result, at positive potentials, for a negative shift of the voltage dependence of current kinetic parameters. Cell 37·3. In *D*, both the activation curve (top), measured at 20 mV with a protocol similar to that used in *B* and *C*, and the fully activated *I–V* relation (bottom) were plotted at the start of an experiment (control) and after 5 min and 7 min, respectively. Run-down appears in this case to affect both the position of the activation curve and the current amplitude. Cell 36.2.

activation. Indeed from the data in Fig. 13 it appears that either a 10-fold decrease (*A*) or a 12-fold increase (*B*) in the pulse frequency do not decelerate or accelerate, respectively, the current decay. The lack of use dependence of current run-down was confirmed in five further experiments similar to those shown in Fig. 12.

A strong acceleration of i_f run-down was observed, on the other hand, in association

with the current increase induced by high K, as shown in Fig. 14. Fig. 14A shows a train of current traces recorded on pulsing to -100 mV during the change from a control 5·4 mM-K to a 25 mM-K solution. After the initial current increase induced by high K, the current begins to fall with a run-down rate higher than in normal K. In some cases we also found that the acceleration of current reduction was such that the current quickly decreased to values smaller than in the control solution. An example of this is illustrated in another experiment in Fig. 14B. Here we applied 0·5 s pulses to -108 mV during perfusion with either 5·4 or 30 mM-K Tyrode. Plotting the current amplitude against time shows that this declined slowly in the control solution and then increased, as expected, on raising the external K concentration to 30 mM. This was followed, however, by an abrupt acceleration of run-down that rapidly brought the current size to values smaller than in control. On return to the control 5·4 mM-K solution, the current was further depressed and kept decreasing with a run-down rate comparable to the initial one.

The behaviour shown in Fig. 14 was observed several times and, although i_f tended to disappear more quickly in high-K solutions, the actual run-down rate varied greatly from cell to cell. As mentioned above this phenomenon complicates the analysis of the effects of K (as well as of Na and Cs) on i_f and makes an accurate quantitative comparison between fully activated I–V relations in different conditions unreliable.

Although the results in Fig. 12 demonstrate that the fully activated i_f does vary with time, some of the data suggest that the voltage dependence of current activation could also be influenced by run-down. From the records in Fig. 12A, for example, it is clear that higher negative pulses have to be applied in order to activate i_f after longer periods of whole-cell recording. As shown in the experiments in Fig. 15, a more detailed analysis of this aspect of current run-down shows that the i_f activation curve is indeed greatly affected by this process.

In Fig. 15A, while the current recorded on stepping to near the half-activation range (-70 mV) declined with time, that elicited by a further step to -100 mV increased, indicating a shift of the activation curve to more negative voltages (compare with Fig. 11B). Negative displacement of the i_f activation curve due to run-down were measured in the experiments shown in Fig. 15B, C and D. In C the activation curve shifted by about -11 mV in the first 8 min from the start of whole-cell recording, and kept shifting as apparent from the partial measurements made after 11 and 17·5 min. This experiment also shows that while the first effect of run-down is a displacement of the i_f activation curve, at later times a depression of its size also occurs, indicating a reduction of the current fully activated amplitude. The simultaneous occurrence of both effects was observed in the experiment shown in Fig. 15D. Here the measurement of activation curve and fully activated I–V relation done after 5 and 7 min, respectively, from the reference measurement showed that the former had undergone a shift of about -7 mV and the latter a marked depression. In summary, according to the data shown above the run-down process involves both kinetics and magnitude of i_f. Interestingly, the modification caused by run-down on the i_f kinetics is opposite to that normally caused by adrenaline.

The results presented in this paper indicate that, as in Purkinje cells (Callewaert *et al.* 1984), most of the properties of the hyperpolarizing-activated current, i_f, in cells isolated from the rabbit sino-atrial node area are similar to those described for the same current in cardiac multicellular preparations.

The threshold for i_f activation lies near -40 to -50 mV and the current is fully activated at about -100 mV (Fig. 5). This range is similar to that found in the intact sino-atrial node preparations (Brown, DiFrancesco & Noble, 1979a,b; Brown & DiFrancesco, 1980; Yanagihara & Irisawa, 1980). In spontaneously active cells, it partially overlaps the slow pace-maker depolarization phase (Fig. 2A). We have been unable to find a correlation between pace-maker activity and size of i_f during the course of an experiment in a single cell. This is mostly to be attributed to the difficulty, mentioned in the Methods, in recording spontaneous activity. Some of the variability found in the i_f threshold and more generally in the position of its activation curve on the voltage may be attributed to natural differences in the availability of i_f channels in different cells. Some, however, may be associated with the run-down phenomenon which, as shown in Fig. 15, involves large variations of the position of the i_f activation curve during whole-cell recording. This is discussed more fully below. Current activation and deactivation are sigmoidal functions of time, as shown in Fig. 6. This feature of i_f kinetics has been reported and studied in Purkinje fibres (DiFrancesco, 1984). It is a peculiar property, unusual in currents that, like i_f, do not inactivate. Like other properties of i_f in single cells, this also showed variability and in some cases no clear delay in current onset was visible (Fig. 6D). Again, the strong effect of run-down on i_f kinetics (see Fig. 15) can at least partly account for this behaviour.

The i_f fully activated I–V relation is roughly linear in the range -110 to $+50$ mV (see Figs. 7 and 10) with a slight tendency to rectify in the outward direction (Figs. 8 and 9), as also reported in Purkinje fibres (DiFrancesco, 1981b, 1982). In normal 5·4 mM-KCl Tyrode solution the i_f reversal potential lies in the range -10 to -20 mV, which is consistent with the mixed Na/K ionic nature of the current. The dependence upon external Na (Fig. 8) and external K (Fig. 9) is analogous to that described for i_f in intact sino-atrial node preparations (Brown & DiFrancesco, 1980; DiFrancesco & Ojeda, 1980) and in Purkinje fibres (DiFrancesco, 1981b) and confirms, at least qualitatively, that external K ions, but not Na ions, have an activating-like effect on the current. The current i_f in sino-atrial node cells is blocked by Cs at millimolar concentrations, as apparent in Fig. 10. The block is voltage dependent and resembles that exerted by Cs on i_f in Purkinje fibres (DiFrancesco, 1982) and in Purkinje cells (Callewaert *et al.* 1984). It should be noted that Noma, Morad & Irisawa (1983) have reported that Cs causes a voltage-independent blockade of this current (their i_h) in multicellular sino-atrial node preparations. This apparent discrepancy may be due to the partial voltage range explored by these authors and to the limited resolution of the i_f time course during deactivation. This can occur if the analysis is performed under conditions where, as it may be the case in the intact tissue, the current time course cannot be properly dissected from overlapping components and from the interference of K accumulation/depletion processes.

Addition of adrenaline (or noradrenaline) to the perfusing solution, when effective, increases i_f on pulsing toward the half-activation range and accelerates the rate of current activation on pulsing to more negative levels (Fig. 11). This is in agreement with the well-documented action of catecholamines in Purkinje fibres (Hauswirth, Nobel & Tsien, 1968; Tsien 1974a, b) and in sino-atrial node intact preparations (Brown, DiFrancesco & Noble, 1979a; Noma, Kotake & Irisawa, 1980). The observation that, however, in the majority of cases adrenaline failed to induce any obvious effect on i_f led us to consider the possibility that, in spite of the apparently healthy conditions of cells, enzymatic treatment could have damaged cell membranes and caused a reduction in the number and/or responsiveness of drug receptors. We tend to discard this as the only possible explanation, however, since visual inspection often confirmed that addition of the catecholamine caused contracting cells to accelerate their spontaneous activity and some silent cells to start beating.

A second plausible explanation of the variability in the response to adrenaline, as well as in the other properties of i_f in isolated sino-atrial node cells, is related to the run-down phenomenon described in Figs. 12–15. The presence of a current decay with time could be explained by assuming that the availability of i_f channels to voltage activation depends on the intracellular presence of an unidentified substance. For example, activation of i_f may require energy supply from an energy source that deteriorates with time, although this does not seem to involve adenosine 5'-triphosphate (ATP) directly, since all pipettes contained it. This substance may migrate from the cell to the pipette interior. In this case, its intracellular concentration would decrease with a rate dependent on several random parameters such as the actual membrane opening width and the rate of exchange between pipette and cell interior. The large variability of run-down speed observed would then be directly related to the variability in the rate of intracellular depletion of this substance. It may be interesting to note that i_f run-down has not been reported in previous work on single sino-atrial node cells (Nakayama *et al.* 1984) or Purkinje cells (Callewaert *et al.* 1984). Consistent with the results in this paper is, however, the fact that Nakayama *et al.* (1984) did find a high variability in the size of i_f (see for example their Fig. 11). Also, it is to be expected that run-down does not appear in the two-micro-electrode experiments performed by Callewaert *et al.* (1984), if it is caused by dilution of an unspecified substance in the suction pipette.

Which substance could this be? Ever since the first studies of the 'pace-maker' current in Purkinje fibres, it has been known that its activity is controlled by adrenaline (Hauswirth *et al.* 1968) and that this control is mediated by intracellular adenosine 3',5'-phosphate (cyclic AMP) (Tsien, Giles & Greengard, 1972). The evidence that run-down involves large negative shifts of the i_f activation curve (Fig. 15) strongly favours the view that it is indeed the mechanism controlling the voltage dependence of the current degree of activation – and hence its availability – that is impaired in the cells under study. According to this view, the observed lack of response to adrenaline could thus be attributed to the failure of one or more steps in the chain of events linking the drug – receptor interactions to channel activation. There is however evidence against the hypothesis that cyclic AMP alone is involved in current run-down, as cyclic AMP has been reported to affect the current kinetics and not the fully-activated *I–V* relation (Tsien, 1974b). If this is the case, results of

the type shown in Fig. 10 cannot be simply explained in terms of a time-dependent loss of intracellular cyclic AMP. Furthermore, addition of cyclic AMP and cyclic-AMP-dependent protein-kinase to the pipette solution in preliminary experiments did not prevent the run-down to occur. A second possibility is that i_f channels need some kind of energy supply in order to be available for voltage-dependent activation. As mentioned above, however, the energy required is not likely to be in the form of ATP, because this was present in the pipette.

Whatever mechanism involved, the possible dependence of the availability of i_f channels on the presence of an energy-supplying substance in the cytosol can explain, together with the current run-down, some of the experimental observations of i_f in single cells. For example, the large variations in i_f size may be due to variations in the availability of this substance. Interestingly, cells that lack i_f often show large current fluctuations, sometimes obviously associated with large leak channels, which would favour the loss of intracellular molecules.

The presence of large-conductance channels has been verified several times in the course of this work during records of i_f (see for example the large unitary events in Figs. 2*A* and *C*, 3, 4*A* and *B*, 6*D* and 7*A*). In the present paper these events have not been analysed. However, single channels with slope conductances of more than 300 pS have often been recorded (D. DiFrancesco, unpublished observations) and it has also been observed that appearance of these channels often shortly precedes the cell's death.

A similar explanation may apply to the variability in the i_f kinetic properties (Figs. 2 and 5) which are obviously under the influence of processes subject to run-down (Fig. 15). Also, the reduced ability of high external K concentrations to increase the i_f fully activated conductance may reflect a lack of energy supply for channel activation (Fig. 9*C*), and the increased rate of current run-down that occurs after raising external K (Fig. 14) may be caused by an augmented energy consumption in high K. A similar interpretation applies, as mentioned already, to the reduced responsiveness to adrenaline.

Although it is not the intent of this paper to investigate the details of the current run-down phenomenon, from the data reported here it is difficult to escape the conclusion that the current i_f is probably under control of factors other than the membrane voltage and that some of the properties so far attributed to voltage dependence may indeed be due to the influence of mechanisms involving the metabolic activity of the cell. Further experimentation will be required to clarify the details of the processes controlling the voltage-dependent activation of i_f channels in the isolated sino-atrial node cell.

REFERENCES

BADER, C. R. & BERTRAND, D. (1984). Effects of changes in intra- and extracellular sodium on the inward (anomalous) rectification in salamander photoreceptors. *Journal of Physiology* **347**, 611–631.

BENDUKIDZE, Z., ISENBERG, G. & KLÖCKNER, U. (1985). Ca-tolerant guinea-pig ventricular myocytes as isolated by pronase in the presence of 250 μM free calcium. *Basic Research in Cardiology* **80**, 1–13.

BROWN, H. F. & DIFRANCESCO, D. (1980). Voltage-clamp investigations of membrane currents underlying pace-maker activity in rabbit sino-atrial node *Journal of Physiology* **308**, 331–351.

BROWN, H. F., DIFRANCESCO, D. & NOBLE, S. J. (1979a). How does adrenaline accelerate the heart? *Nature* **280**, 235–236.

BROWN, H. F., DIFRANCESCO, D. & NOBLE, S. J. (1979b). Cardiac pacemaker oscillation and its modulation by autonomic transmitters. *Journal of Experimental Biology* **81**, 174–204.

BYERLY, L. & HAGIWARA, S. (1982). Calcium currents in internally perfused nerve cell bodies of *Limnea stagnalis*. *Journal of Physiology* **322**, 503–528.

CALLEWAERT, G., CARMELIET, E. & VEREEKE, J. (1984). Single cardiac Purkinje cells: general electrophysiology and voltage clamp analysis of the pace-maker current. *Journal of Physiology* **349**, 643–661.

COHEN, I. S., FALK, R. T. & MULRINE, N. K. (1983). Actions of barium and rubidium on membrane currents in canine Purkinje fibres. *Journal of Physiology* **338**, 589–612.

DATYNER, N. B., GINTANT, G. A. & COHEN, I. S. (1985). Microprocessor controlled trituration device for the dissociation of cardiac and other tissues. *Pflügers Archiv* **403**, 105–108.

DIFRANCESCO, D. (1981a). A new interpretation of the pace-maker current in calf Purkinje fibres. *Journal of Physiology* **314**, 359–376.

DIFRANCESCO, D. (1981b). A study of the ionic nature of the pace-maker current in calf Purkinje fibres. *Journal of Physiology* **314**, 377–393.

DIFRANCESCO, D. (1982). Block and activation of the pace-maker channel in calf Purkinje fibres: effects of potassium, caesium and rubidium. *Journal of Physiology* **329**, 485–507.

DIFRANCESCO, D. (1984). Characterization of the pace-maker current kinetics in calf Purkinje fibres. *Journal of Physiology* **348**, 341–367.

DIFRANCESCO, D. (1985). The cardiac hyperpolarizing-activated current, i_f. Origins and developments. *Progress in Biophysics and Molecular Biology* **46**, 163–183.

DIFRANCESCO, D. & FERRONI, A. (1983). Delayed activation of the cardiac pacemaker current and its dependence on conditioning prehyperpolarizations. *Pflügers Archiv* **396**, 265–267.

DIFRANCESCO, D., NOMA, A. & TRAUTWEIN, W. (1979). Kinetics and magnitude of the time-dependent K current in the rabbit SA node: effect of external potassium. *Pflügers Archiv* **381**, 271–279.

DIFRANCESCO, D. & OJEDA, C. (1980). Properties of the current i_f in the sino-atrial node of the rabbit compared with those of the current i_{K2} in Purkinje fibres. *Journal of Physiology* **308**, 353–367.

EARM, Y. E., SHIMONI, Y. & SPINDLER, A. J. (1983). A pace-maker-like current in the sheep atrium and its modulation by catecholamines. *Journal of Physiology* **342**, 569–590.

FENWICK, E. M., MARTY, A. & NEHER, E. (1982). Sodium and calcium channels in bovine chromaffin cells. *Journal of Physiology* **331**, 599–635.

HALLIWELL, J. V. & ADAMS, P. R. (1982). Voltage clamp analysis of muscarinic excitation in hippocampal neurones. *Brain Research* **250**, 71–92.

HAMILL, O. P., MARTY, A., NEHER, E., SAKMANN, B. & SIGWORTH, F. J. (1981). Improved patch-clamp techniques for high-resolution current recording from cells and cell-free membrane patches. *Pflügers Archiv* **391**, 85–100.

HART, G., NOBLE, D. & SHIMONI, Y. (1980). Adrenaline shifts the voltage dependence of the sodium and potassium components of i_f in sheep Purkinje fibres. *Journal of Physiology* **308**, 34P.

HAUSWIRTH, O., NOBLE, D. & TSIEN, R. W. (1968). Adrenaline: mechanism of action on the pacemaker potential in cardiac Purkinje fibres. *Science* **162**, 916–917.

ISENBERG, G. & KLÖCKNER, U. (1982). Calcium tolerant ventricular myocytes prepared by preincubation in a KB medium. *Pflügers Archiv* **395**, 6–18.

LÖFFELHOLZ, K. & SCHOLZ, H. (1970). Inhibition of Mn^{++}-catalyzed autoxidation of adrenaline by ascorbic acid. *Experientia* **26**, 637–638.

MAYER, M. L. & WESTBROOK, G. L. (1983). A voltage-clamp analysis of inward (anomalous) rectification in mouse spinal sensory ganglion neurones. *Journal of Physiology* **340**, 19–45.

MAYLIE, J. & MORAD, M. (1984). Ionic currents responsible for the generation of pace-maker current in the rabbit sino-atrial node. *Journal of Physiology* **355**, 215–235.

NAKAYAMA, T., KURACHI, Y., NOMA, A. & IRISAWA, H. (1984). Action potential and membrane currents of single pacemaker cells of the rabbit heart. *Pflügers Archiv* **402**, 248–257.

NOBLE, D. & TSIEN, R. W. (1968). The kinetics and rectifier properties of the slow potassium current in calf Purkinje fibres. *Journal of Physiology* **195**, 185–214.

NOMA, A. & IRISAWA, H. (1976). Membrane currents in the rabbit sinoatrial node cell as studied by the double microelectrode method. *Pflügers Archiv* **366**, 45–52.

NOMA, A., KOTAKE, H. & IRISAWA, H. (1980). Slow inward current and its role mediating the chronotropic effect of epinephrine in the rabbit sinoatrial node. *Pflügers Archiv* **388**, 1–9.

NOMA, A., MORAD, M. & IRISAWA, H. (1983). Does the 'pacemaker current' generate the diastolic depolarization in the rabbit SA node cells? *Pflügers Archiv* **397**, 190–194.

NOMA, A., YANAGIHARA, K. & IRISAWA, H. (1977). Inward membrane currents in the rabbit sino-atrial node cell. *Pflügers Archiv* **372**, 43–51.

PEPER, K. & TRAUTWEIN, W. (1969). A note on the pacemaker current in Purkinje fibres. *Pflügers Archiv* **309**, 356–361.

POWELL, T., TERRAR, D. A. & TWIST, V. W. (1980). Electrical properties of individual cells isolated from adult rat ventricular myocardium. *Journal of Physiology* **302**, 131–153.

POWELL, T. & TWIST, V.W. (1976). A rapid technique for the isolation and purification of adult cardiac muscle cells having respiratory control and a tolerance to calcium. *Biochemical and Biophysical Research Communications* **72**, 327–333.

TANIGUCHI, J., KOKUBUN, S., NOMA, A. & IRISAWA, H. (1981). Spontaneously active cells isolated from the sinoatrial and atrioventricular nodes of the rabbit heart. *Japanese Journal of Physiology* **31**, 547–558.

TSIEN, R. W. (1974a). Effect of epinephrine on the pacemaker potassium current of cardiac Purkinje fibres. *Journal of General Physiology* **64**, 293–319.

TSIEN, R. W. (1974b). Mode of action of chronotropic agents in cardiac Purkinje fibres. *Journal of General Physiology* **64**, 320–342.

TSIEN, R. W., GILES, W. & GREENGARD, P. (1972). Cyclic AMP mediates the effects of adrenaline on cardiac Purkinje fibres. *Nature* **240**, 181–183.

YANAGIHARA, K. & IRISAWA, H. (1980). Inward current activated during hyperpolarization in the rabbit sinoatrial node cell. *Pflügers Archiv* **385**, 11–19.